Appl. Phys. B 92, 93–98 (2008)
DOI: 10.1007/s00340-008-3053-z

Applied Physics B
Lasers and Optics

Intermittent curing and its effect on pulsed laser-induced photopolymerization

X. SUN[1]
D. YIN[1]
H. DAI[1]
J. LIU[1,✉]
R. LU[2]
S.-T. WU[2]

[1] State Key Lab for Advanced Photonic Materials and Devices, Department of Optical Science and Engineering, Fudan University, Shanghai 200433, P.R. China
[2] College of Optics and Photonics, University of Central Florida, Orlando, FL 32816, USA

Received: 30 March 2008/Revised version: 17 April 2008

ABSTRACT Different intermittent curing methods were conducted for pulsed laser induced photopolymerization reactions in a TMPTA acrylic system. Two methods of curing were compared, named grouped pulses impingement (GPI) and consecutively pulsed curing (CPC), respectively, in which the total number of the curing pulses were kept same. In GPI, a prominent light diffraction effect was observed in the post curing process, but was absent in the CPC procedure. A condensed but limited sized core of polymeric structure was the cause of the light diffraction. The amount of inhomogeneity in the refractive index for the core was about 90% of the cured background. Simulations based on Fresnel diffraction theory were performed, and the result was in good agreement with the experimental observations.

PACS 42.25.Bs; 61.82.Pv; 82.35.-x

1 Introduction

In photo induced free radical polymerization (FRP) [1], the reaction is initiated by free radical molecules in the components of the syrup. Functional groups like carbon–carbon double bonds in monomer molecules are then opened by these energetic radicals, and monomeric or oligomeric radicals are then formed and polymerized instantly or successively to construct large polymeric molecules [2]. If the sample is exposed to curing light with an inhomogeneously distributed intensity, the conversion of monomer into polymer in brighter areas would be more than that at darker ones. Monomeric or oligomeric molecules in the darker areas will usually diffuse into brighter areas due to the concentration gradients, and therefore the reactions of polymerization could be sustained to some extent.

The prevailing theory, on the construction of inhomogeneous structure due to inhomogeneous photopolymerization, was first proposed by Zhao [3], in photo curable materials with holographic curing. The resultant inhomogeneity in the film, presented by the relatively aggregated sections of polymer and monomers, could be described in terms of the difference in refractive index between polymer and monomer. In Zhao's model, the reaction rate of the photopolymerization was assumed to be linearly proportional to the curing light intensity, whereas half order dependence has also been proposed [4]. This phenomenological model was also modified by the addition of the effective void concentration in order to keep the conservation for mass distributions in the sample, on account of polymerization induced shrinkage or contraction during reactions [5].

One of the most important features in photo induced FRP is post curing polymerization [1], that is, when initiated above the threshold, polymerization reactions will continue to go on even if the curing light has been turned off, though the reaction rate would be different from that with the curing light on. This post curing effect was not included in Zhao's or the subsequent theories on photopolymerization. In contemporary methods for dynamical measurements on photopolymerization, such as real-time infrared (RTIR) spectroscopy [6], information on molecular structural changes is monitored as the cursor of the extent of the polymerization reaction. However, dynamical properties in the macro scale, such as molecular diffusion, are usually neglected, which might be of substantial importance for HPDLC based optical devices [7, 8].

In order to investigate the dynamic process of the structural change during photopolymerization in the sample film, we report in this paper, the experimental observations of the dynamical behavior of pulsed laser induced photopolymerization (PLP) in a TMPTA acrylate crosslinking system by intermittent curing. Two methods of curing have been conducted, named grouped pulses impingement (GPI) and consecutively pulsed curing (CPC), respectively. Different results were observed, showing that different structures were formed in the sample films in the two different curing processes. In GPI, a prominent light diffraction effect was observed in the post curing process, whereas it was absent in the CPC procedure. Simulations, based on Fresnel diffraction theory, demonstrate a condensed but limited sized core of polymeric structure, therefore the inhomogeneity in refractive index, was the cause of the light diffraction. The result is in good agreement with the experimental observations.

✉ Fax: +86-21-65642134, E-mail: jhliu@fudan.edu.cn

2 Theory and experiments

According to the reaction-diffusion model [3–5], a method that could trace up the dynamical process macroscopically for the photopolymerizaton reaction has been proposed [9], which is briefly outlined hereafter. Photopolymerization starts up by the initiation of free radicals which are produced by the curing photons of appropriate intensity and energy. Monomers are converted into polymer during the reaction. Regarding the processes of the variations for components in polymerization reactions, a one dimensional model is a simple method of description.

Assuming a sample film is being cured by a light with certain spatial distribution, the concentration of monomer molecules at a certain position in the sample, represented by $\varphi_i^{\mathrm{m}}(x,t)$, and $\varphi_i^{\mathrm{p}}(x,t)$ as that of the produced polymer, can be described as functions of time by [3, 8]:

$$\frac{\partial\varphi_i^{\mathrm{m}}(x,t)}{\mathrm{d}t}=\frac{\partial}{\partial x}\left(D_i(x,t)\frac{\partial\varphi_i^{\mathrm{m}}(x,t)}{\partial x}\right)-F_i(x,t)\varphi_i^{\mathrm{m}}(x,t)\,, \quad (1)$$

$$\frac{\partial\varphi_i^{\mathrm{p}}(x,t)}{\mathrm{d}t}=F_i(x,t)\varphi_i^{\mathrm{m}}(x,t)\,, \quad (2)$$

where $D_i(x,t)$ and $F_i(x,t)$ are the monomer diffusion coefficient and reaction rate, respectively. x and t are 1D spatial and time coordinates, respectively.

Concentrations $\varphi_i^{\mathrm{m}}(x,t)$ and $\varphi_i^{\mathrm{p}}(x,t)$ could be obtained by solving the above equations if the diffusion coefficient and rate parameter are known. Polymerization reactions would cause a higher density at positions with more polymers than that with more monomers. Due to the difference for polymer and monomer in terms of refractive index, a certain pattern of the curing light would produce a corresponding distribution of the inhomogeneity in the sample film, resulting in light diffraction or scattering where a beam of probing light shines.

If a Gaussian distributed curing light, which is easier to obtain from the fundamental mode of a laser output, is used to induce the photopolymerization, the variation of refractive index $\Delta n(r,t)$ would be proportional to the Gaussian intensity profile in space, according to Zhao [3]. Therefore, the refractive index of the cured area could be expressed phenomenologically as:

$$n(r,t)=n_0+\delta n(t)\exp\left(-2r^2/w_{\mathrm{c}}^2\right)\,, \quad (3)$$

where n_0 is the refractive index of background monomer, the exponential function in (3) stands for the Gaussian intensity distribution of the curing laser on the sample film, and $\delta n(t)$ is the amplitude of the refractive index variation in the cured areas, which representing the mixture of monomer and polymer.

Thus the sample film, whose refractive index profiling transversely as a function of Gauss, will act as a lens-like media, through which a transmitted probing laser beam would encounter a focusing or defocusing effect. By detecting the transmitted probe light through an iris at a certain distance downstream from the position of the sample film, as similar to the Z-scan method [10], the dynamical process of the structural variation in the polymerization reaction in the cured area, can be followed in real time. The amplitude of the refractive index variation $\delta n(t)$can therefore be traced [9].

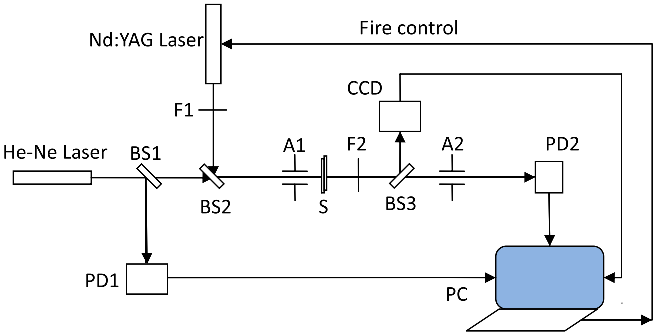

FIGURE 1 Schematic diagram of the experimental setup: F – filter; BS – beam splitter; A – aperture; S – sample; PD – photodetector; PC – personal computer

In this paper, a home made frequency doubled pulsed Nd:YAG laser was adopted as the curing light source, the transverse mode of the laser pulses was restricted to the fundamental by a cavity iris, so that the light intensity could be a Gaussian type. The laser firing is controlled by a computer, so that the repetition rate and number of the pulses to be fired can be preset at will. In the experiments, the pulse repetition rate was chosen as 20 Hz, pulse energy was measured to be 0.04 mJ, and the pulse width was about 100 ns (FWHM). The averaged pulse intensity density was therefore about 60 mW/cm^2. The sample syrup, as formulated in [9], consisted of, in a ratio of weight percentage, 62% trimethylolpropane triacrylate monomer, 25% N-vinylpyrrollidone (NVP), 1.8% N-phenylglycine (NPG), and 1.2% Rose Bengal (RB), all were from Aldrich. The sample syrup was filled into an ITO coated glass cell of 20 μm thickness.

The experimental setup is schematically illustrated in Fig. 1. In the experiment, two methods of pulsed laser exposures were conducted, with the total numbers of curing pulses fixed. One was consecutively pulsed curing (CPC), in which a preset number of pulses were fired completely at a certain repetition frequency. The other one was grouped pulses impingement (GPI), in which laser pulses were fired in groups with some certain time intervals, depending on the stages of the polymerization reactions. During exposures for the two methods, there was a slender weak He-Ne laser beam, with a Gaussian intensity distribution, passing coaxially through the cured area of the sample film, probing the structural variation in the process of polymerization. This is represented by the transmittance change for the He-Ne laser through an iris at a certain distance downstream from the position of the cured sample. Meanwhile a CCD camera, Panasonic wv-CP410/G, with an effective sensor area of $4.8\times3.6\,\mathrm{mm}^2$, and positioned at the same distance from the film as that of the iris, monitored the probe beam profile that passed through the sample film in real time.

3 Results and discussions

A typical trace of the transmittance of the probe laser beam through the second iris A2 as a function of time is illustrated in Fig. 2, for which the sample was consecutively shot by 100 pulses of the 532 nm Nd:YAG laser at

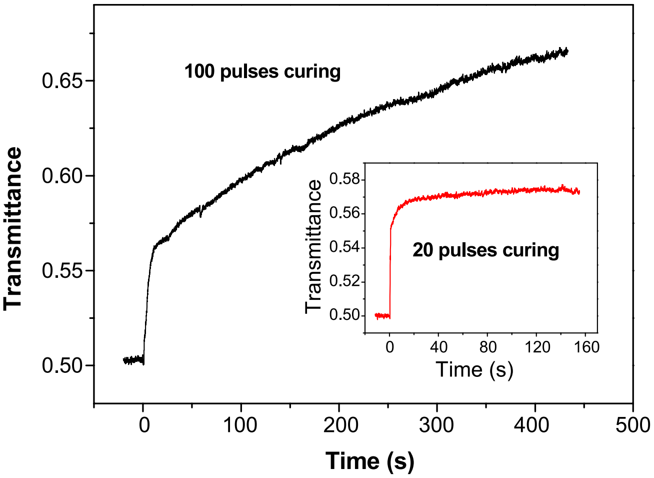

FIGURE 2 Transmittance as a function of time for the photopolymerization processes with an exposure of 100 pulses at 20 Hz. *Insert*: CPC exposure with 20 pulses

FIGURE 3 Probing beam image of the He-Ne laser snap shot by CCD, 150 s after the sample was cured by CPC with a total of 20 laser pulses

a repetition rate of 20 Hz. During a time interval of about 5 s when curing pulses were launched, the transmittance of the He-Ne laser increased rapidly from 0.5 to 0.56 at a speed of 0.0059 s^{-1}. This was the period of photopolymerization reaction initiated by laser induced free radicals. The increment of the transmittance was due to axially symmetric aggregations of the monomeric and polymeric mixture in the sample cell caused by the Gaussian profiled pulsed laser curing. Diffusion of monomeric molecules in the process of polymerization reaction played an important role. After pulse firing was completed, the transmittance still increased, but at a slower speed of about 0.0002 s^{-1}. During an experimental time that spanned 450 s, the post-curing effect was prominent such that photopolymerization, or in other words, aggregation of monomeric and polymeric molecules, continued and made the sample film contract centrosymmetrically. The film thereafter acted as a lens like media that could focus more of the probe He-Ne laser through the iris A2, and consequently resulted in a transmittance increase.

Quantitatively, each point on the transmittance curve can be converted to the amplitude of the variation of the refractive index ($\delta n(t)$) in the cured film, by means of the method proposed in [9]. Here for example, we figured out the $\delta n(t)$ for the last point in the curve of Fig. 2, which is about 0.02, i.e. about 1.4% increment compared with n_0 for the background monomer. It is evident that the post curing effect, which is a well-known phenomena [1], is however absent in the reaction-diffusion theory as simplified by Zhao [3].

The insert in Fig. 2 shows the transmittance curve for the probe He-Ne laser through a sample film that was cured with a total number of 20 pulses (1 s curing time) by CPC exposure. During curing, photopolymerization reactions resulted in a transmittance jump at a speed of 0.071 s^{-1}. Afterwards, the post curing effect continued at a much slower speed of 7×10^{-4} s^{-1}, but was still evident. Transmittance became stable 10 s after the curing, showing that the polymerization reaction ceased in the film thereafter. The amplitude of the refractive index inhomogeneity $\delta n(t)$ at the end of the experiment was about 0.01. Figure 3 is the CCD image of the probe beam snapped 150 s after the curing, and it shows no evident deformation from the Gaussian profile for the wave front of the probe beam.

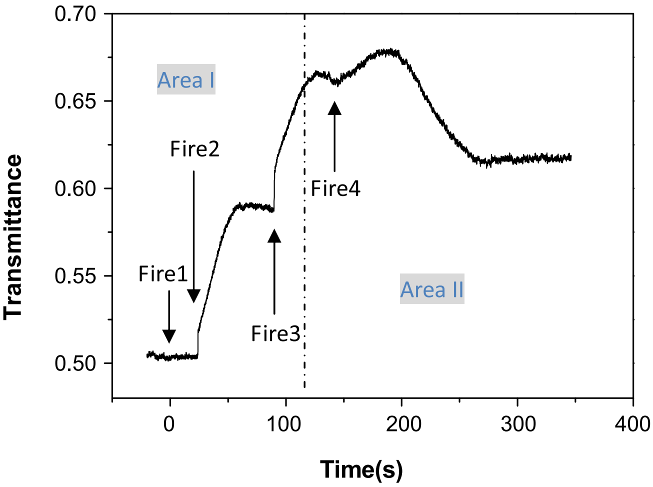

FIGURE 4 Transmittance as a function of time for the photopolymerization in the sample cured by GPI, with a total of 20 pulses in 4 groups, launched at 0, 24, 89, and 147 s, respectively

Figure 4 is the transmittance of the probe beam through the sample by grouped pulses impinging (GPI) curing, with a total of 20 pulses, which reveals a different behavior of photopolymerization reaction in the sample film. In order to make the explanations more clear, Fig. 4 is divided into two parts, or timewise, from the beginning to 130 s, named Area I, and the remaining part is Area II.

In Area I, at the time origin when the sample was shot by the first group of 5 pulses at a repetition rate of 20 Hz, no evident change for the transmittance of the probe beam could be observed. This was the induction period [11], during which the photo induced free radicals was insufficient to induce the photopolymerization in the sample syrup. After about 24 s, the second group of 5 pulses was fired, and there was a rapid increase in the transmittance with a slope of 0.016 s^{-1}, and a post curing polymerization followed with a slope of 0.0024 s^{-1}. Polymerization continued in the dark and saturated within 30 s. At 89 s after the beginning, the third group of 5 pulses was launched, and a similar variation in probe beam transmittance was observed, again another post curing reaction succeeded. The amplitude of transmittance went up to about 0.66, well above the CPC induced transmittance of around 0.6. After a small hump appeared, transmittance then went down slightly. The final group of 5 pulses was then beamed onto the sample, and a slow increase in the transmittance was observed till it reached a maximum of 0.68. Afterwards the transmittance decreased to about 0.62, and became stable thereafter.

An intensity ring could be observed by the naked eye on the surface of the iris A2, showing that the decrease of transmittance was due to diffraction of the probe beam as it was passing through the cured film. The intensity of the diffraction ring was too dim to be recorded directly by the CCD if the total beam profile was included. By sacrificing the large saturation of the CCD sensibility on the central portion of the probe beam, the image of the diffraction ring could then be recorded as shown in Fig. 5, though with some interference noise. The brightest white portion in the image was due to the strong saturation of the pixels of the CCD camera by the central part of the probe beam.

In order to figure out the reason for the diffraction ring, an assumption and subsequent simulations were made based on Fresnel diffraction theory [12]. According to the reaction-diffusion model, inhomogeneous structure in the macroscopic scale, or inhomogeneity in the refractive index, could be linked to the spatial profile of the curing light intensity. Consequently, in this paper, an inhomogeneity of the Gaussian profile in the refractive index was assumed to have developed during the first three groups of curing pulses. Due to the separated impingements of grouped pulses, reacting monomer or monomeric radicals had time to reconfigure or relax gradually in the intervals of the curing, so that a denser part of the mixed structure of monomeric and polymeric networks could be formed. Moreover, the active tri-carbon–carbon double bonds in the TMPTA molecule could further facilitate the polymerization reactions by crosslinking. Thus a denser core of polymer that could diffract the probe laser beam is reasonably assumed to be created in the central part of the cured area, where the curing light intensity, and therefore the reaction rate was a maximum.

The core is assumed to be an additional inhomogeneous structure in the refractive index, also with a Gaussian profile which superpositioned with the background polymeric structure. The refractive index distribution laterally across the cured area could then be represented as the following:

$$n(r,t) = n_0 + \delta n(t)\exp\left(-2r^2/w_\mathrm{c}^2\right) + \eta(t)\exp\left(-2r^2/w_\eta^2(t)\right) . \tag{4}$$

The first two items on the right hand side of (4) are the same as in (3), representing, respectively, the refractive index distribution of background monomer and the curing produced polymer. In the third term of (4), $\eta(t)$ and $w_\eta(t)$ stands for the amplitude and radius of the refractive index profile of polymeric core.

In order to simulate the diffraction of the probe beam by this polymeric core, an input probing light is assumed to have a field strength of

FIGURE 5 Probing beam image of the He-Ne laser snap shot by CCD 150 s after the fourth grouped pulses exposure on the sample film

$$U_i(x_i) = \exp\left(-x_i^2/w_\mathrm{p}^2\right) ,$$

with 1D Gaussian distribution, and with coordinates and beam width as x_i and w_p, respectively. The transmitted field strength through the sample could be expressed as [12]: $U_t(x_i) = T(x_i)U_i(x_i)$, where $T(x_i)$ is the transmittance function of the sample film being cured. The absorption to the probe light in the sample syrup was negligible in our case [9], $T(x_i)$ is therefore a phase-only function, which could be expressed as $T(x_i) = \mathrm{e}^{(jkn(x_i)d)}$, where $k = 2\pi/\lambda$ is the wave vector of the probe beam, d is the sample thickness, and j is the imaginary unit. According to Fresnel diffraction theory, the 1D field strength at the observation plane of iris A2, z distance downstream from the sample position, could be expressed as [12]:

$$U_\mathrm{o}(x_\mathrm{o}) = \frac{\exp(jkz)}{j\lambda z}\int_\infty U_t(x_i)\exp\left\{j\frac{k}{2z}[x_\mathrm{o}-x_i]^2\right\}\mathrm{d}x_i , \tag{5}$$

where x_o are the coordinates at the observation plane.

The intensity profile at the observation plane would be proportional to $|U_\mathrm{o}(x_\mathrm{o})|^2$. With a transmittance of about 0.7 for this experiment, δn could be calculated to be about 0.02. Assuming that the amplitude $\eta(t)$ and radius w_η of the core could vary at some certain ranges, $|U_\mathrm{o}(x_\mathrm{o})|^2$ could then be calculated with the help of (4) and (5), together with the transmittance function $T(x_i)$. Result is shown in Fig. 6. Parameters used in the calculation were based on the experimental conditions, including curing beam width, $w_\mathrm{c} = 0.65$ mm, $\delta n(t) = 0.02$, $w_\mathrm{p} = 0.15$ mm, $z = 570$ mm, $\lambda = 632.8$ nm, $d = 20\,\mu$m, and the observation plane was taken to be an area of 5×5 mm^2.

The prominent feature in Fig. 6 for the calculated light intensity distribution on the observation plane is a main hump with two small sidelobes on both sides. In other words, for the 2D situation, it would be a main intense central part of probe beam surrounded by only one distinct ripple ring, whose intensity is about 10% of the main peak in this case. This is qualitatively in agreement with the CCD image in Fig. 5.

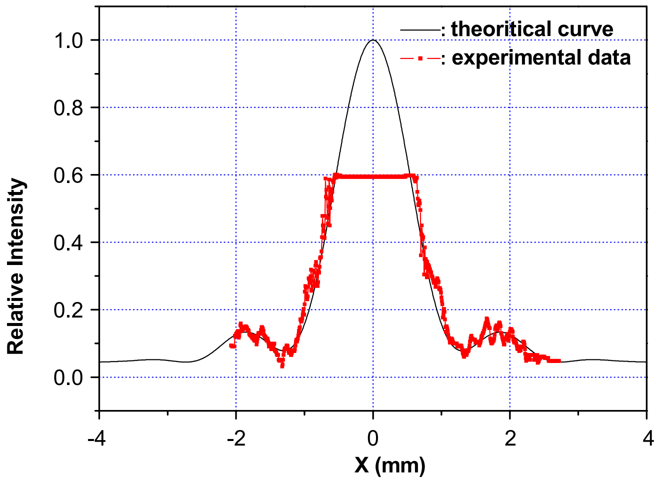

FIGURE 6 Relative intensities of the theoretical and experimental profiles of the probe beam. The polymeric core parameters are set as $\eta = 0.018$, $w_\eta = 0.1 w_\text{p}$, $w_\text{p} = 0.15$ mm, respectively

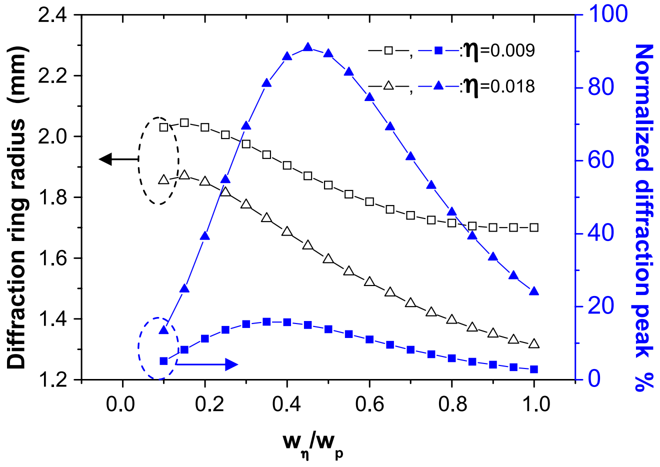

FIGURE 7 Calculated diffraction properties as a function of the core size with the core amplitude as a constant parameter, for details see the text

For comparison purposes, the central transverse intensity profile of image in Fig. 5 was rescaled and put into Fig. 6. The two curves match well. Quantitative data that could be retrieved from the image in Fig. 5 are the radii of the main beam, $r_\text{p} = 1.32$ mm, the distance from the beam center to the first minimum of intensity, and for the diffraction ring, $r_\text{r} = 1.79$ mm, the separation from the center to the intensity maximum of the diffraction ring. These two values were obtained from the experimental intensity profile in Fig. 6 by means of appropriate smoothing, which is not shown in Fig. 6.

The theoretical curve in Fig. 6 was produced by parameters, $\eta(t) \approx 0.018 = 90\% \delta n$, and $w_\eta = 0.1 w_\text{p}$, which were chosen from one of large numbers of simulations, for it could match the experimental profile, with a tolerance of 3% between the calculated and the smoothed values of r_p and r_r. The total amount of change in amplitude of refractive index, $\eta(t) + \delta n(t)$, is 0.038, which almost equals to 0.039, the difference in refractive index from our separate measurements on monomer and polymer, respectively.

Variations of the radius of the diffraction ring, and its intensity as a percentage of that of the main beam, are numerically simulated as functions of $\eta(t)$ and w_η. It could be seen in Fig. 7 that, with constant $\eta(t)$, r_r diminishes monotonically as the size of the core increases, whereas the diffraction intensity has a maximum at about 40% of the probe beam size w_p. In Fig. 8, if w_η is fixed, the diffraction intensity goes up monotonically as $\eta(t)$ increases, whereas the ring diminishes towards the center of the beam.

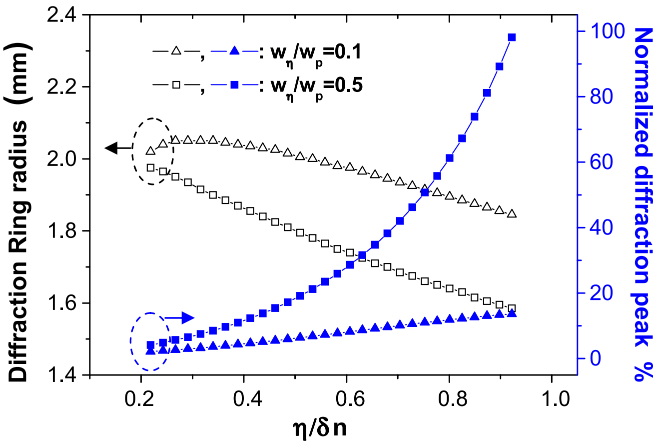

FIGURE 8 Calculated diffraction properties as a function of the core amplitude with the core size as a constant parameter, for details see the text

The probe beam image in Fig. 5 was taken at the same distance from the sample film with respect to the iris A2 in the experiment. Although the sensor area of the CCD used was not big enough to snap more spatial range, it did not prevent us from observing the beam pattern on the plane of the iris by eye. There was only one significant diffraction ring that could be seen on the iris A2 during the experiment, which was in good agreement with the simulated result as in Fig. 6. Therefore an inhomogeneous core induced light diffraction is the reason for the transmittance decrease in the GPI method, as well as the formation of the diffraction ring.

Therefore according to our experiments, different intermittent curing processes in photopolymerization can cause different polymeric structures due to the different reaction and propagation rates of the monomer or polymeric radicals, or termination mechanisms [13]. Given the same total curing energy, no such diffraction was observed in the CPC procedure. Therefore the formation of a protruding core structure clearly demonstrated that the post-curing effect plays an important role in the construction of a polymeric network, or macroscopic structure, in photopolymerization reactions. The significance, on the theoretical part, of our experiments, is that the current reaction-diffusion model of photopolymerization should have to be modified to include the post curing effect, in order to be more precise in predicting the process and final structure of photopolymerization reactions.

Realistically, the formation of macroscopically denser structures in the polymeric network during polymerization reactions would further exhaust the structural voids that could accommodate small molecules such as liquid crystal molecules, and consequently facilitate a more complete phase separation between small molecules and polymer, like in HPDLC. Thus, by means of modifications of curing processing, intermittently for example, more promising performances in optical devices made from HPDLC can be expected [14, 15].

4 Conclusions

Pulsed laser induced photopolymerization by means of intermittent curing could play an important role in modifying the microscopic or macroscopic structure of a polymeric network. Two different exposure methods, consecutively pulsed curing (CPC) and grouped pulses impingement (GPI), have been conducted on a TMPTA acrylate system. With the same total energy of curing, different amplitude increases in the refractive index in photopolymerization reactions were obtained, 0.01 for CPC, and 0.02 for GPI, respectively. Moreover a distinct diffraction of the probing beam in the GPI procedure was observed, which was attributed to the generation of a denser core of polymeric structure in the cured area in the sample. The core was modeled as an additional Gaussian shaped increment in the refractive index profile, 90% of that of the cured polymeric structure. The model and corresponding calculations were in reasonable agreement with experimental observations.

ACKNOWLEDGEMENTS This work is sponsored by the National Science Foundation of China, approval number 10574031.

REFERENCES

1 C. Decker, Macromol. Rapid Commun. **23**, 1067 (2002)
2 G. Odian, *Principles of Polymerization* (Wiley, New York, 2004), 4th edn.
3 G.H. Zhao, P. Mouroulis, J. Mod. Opt. **41**, 1929 (1994)
4 J. Qi, J. Appl. Phys. **96**, 2443 (2004)
5 J. Qi, J. Appl. Phys. **91**, 4795 (2002)
6 C. Decker, K. Moussa, Macromolecules **22**, 4455 (1989)
7 R.L. Sutherland, L.V. Natarajan, V.P. Tondiglia, T.J. Bunning, Chem. Mater. **5**, 1533 (1993)
8 V.L. Colvin, R.G. Larson, A.L. Harris, M.L. Schilling, J. Appl. Phys. **81**, 5913 (1997)
9 F. Wang, B. He, X. Sun, H. Dai, J. Liu, Appl. Phys. B **86**, 117 (2007)
10 M. Sheik-Bahae, A.A. Said, T. Wei, D.J. Hagan, E.W. Van Stryland, IEEE J. Quantum Electron. **QE-26**, 760 (1990)
11 C. Decker, A.D. Jenkins, Macromolecules **18**, 1241 (1985)
12 J.W. Goodman, *Introduction to Fourier Optics* (McGraw-Hill, New York, 1968)
13 C. Barner-Kowollik, M. Buback, M. Egorov, T. Fukuda, A. Goto, O.F. Olaj, G.T. Russell, P. Vana, B. Yamada, P.B. Zetterlund, Prog. Polym. Sci. **30**, 605 (2005)
14 R. Caputo, L. De Sio, A. Veltri, C. Umeton, Opt. Lett. **29**, 1261 (2004)
15 A. d'Alessandro, R. Asquini, C. Gizzi, R. Caputo, C. Umeton, A. Veltri, A.V. Sukhov, Opt. Lett. **29**, 1405 (2004)